Modelling of Hot Water Buffer Tank and Mixing Loop for an Intelligent Heat Pump Control

Imran Riaz Hasrat, Peter Gjøl Jensen, Kim Guldstrand Larsen, and Jiří Srba

Department of Computer Science, Aalborg University, Denmark
{imranh, pgj, kgl, srba}@cs.aau.dk

Abstract. The recent surge in electricity prices has increased the demand for cost-effective and sophisticated heat pump controllers. As domestic floor heating systems are becoming increasingly popular, there is an urgent need for more efficient control systems that include also heat buffer tanks to account for fluctuating energy prices. We propose a scalable thermal model of the hot water buffer tank together with a mixing loop and evaluate its operation and performance on an experimental Danish house from the OpSys project. We experimentally assess the buffer tank's quality by selecting the proper size and number of virtual layers using an industry-standard controller. Finally, we integrate the buffer tank and mixing loop into the heating system and create an intelligent STRATEGO controller to examine their performance. We analyze the tradeoff between cost and comfort for different buffer tank sizes to determine when a buffer tank or a mixing loop should be included in the system. By providing a detailed understanding of the buffer tank and mixing loop, our study enables the clients to make better decisions regarding the appropriate buffer tank size and when to install a mixing loop based on their specific heating needs.

Keywords: Intelligent heat pump control · Energy efficiency · Floor heating · Buffer tank modelling.

1 Introduction

According to 2020 figures, Renewable Energy Sources (RESs) contribute up to 26 % in domestic space heating [1]. The proportion of RES in Denmark's electricity market has increased from 44 % in 2015 to 50 % in 2020 with the ultimate objective of becoming carbon-free by 2050 [2].

There is a substantial potential for integrating RES into domestic heating systems to reduce energy consumption costs. Heat pumps enable the heating system to utilize flexible energy. Furthermore, a hot water buffer tank can enhance the heating system's energy flexibility. Integrating a hot water buffer tank can play a key role in improving energy efficiency. The tank model must accurately determine the water temperature inside the tank in order to better exploit the buffer tank. In addition, in modern space heating a mixing loop can be introduced between the water tank and heaters to mix up the hot and cold water to

improve efficiency and provide better regulation of water flow into the heaters. An intelligent heat pump controller is required to maximize the benefits of the buffer tank and the mixing loop.

When used in domestic heating control systems, Model Predictive Controllers (MPC) demonstrated the potential for energy and cost savings [3–5]. An estimated house model depicting the thermal dynamics of the house is required before developing an MPC. The thermodynamics model depicts the house's heat dynamics as well as the impacts of outdoor weather, residents' behaviour, and solar radiation on the room temperature. Given the thermodynamics model, an MPC is coupled with a control objective (e.g., reduce cost and optimize comfort) in a tight and periodic loop of "observe, solve, act." However, implementing an MPC has various challenges, such as the house dynamics needing to be discovered in advance and the behaviour and dynamics changing over time.

To tackle these issues, we use the control setup from our recent work [6], where we first identify the thermodynamics and heat transfer coefficient using CTSM-R (continuous time stochastic modelling in R) [7], and then design an intelligent Uppaal Stratego [8] controller, which controls the heat pump for the floor heating using an online strategy synthesis approach. In this paper, we additionally propose and implement thermodynamic models of the hot water buffer tank and the mixing loop. We incorporate the models into the heating system and create intelligent Stratego controllers to operate it. Our main novel contributions are:

1. Development of a dynamic thermal model of the hot water buffer tank.
2. Quality assessment to examine the impact of virtual layers and tank sizes.
3. Integration of a mixing loop for mixing hot and cold water to achieve more flexibility and better control of forward water temperature.
4. Employment of the heat buffer tank and mixing loop models to design the Stratego MPC.
5. Extensive experimental evaluation.

Related Work: Recently, emerging studies on domestic heating systems yielded some particularly compelling findings. For instance, a study published in [9] optimized energy costs in an ultra-low temperature district heating system using an MPC for a 22-flat building in Copenhagen, demonstrating significant energy savings. Another study [10] suggested an online and compositional synthesis approach by employing Stratego controller for comfort optimization in a domestic floor heating problem. Similarly, [6] proposed a toolchain for controlling heat pump operation in a floor heating system, specifically for optimal cost and comfort optimizations. In this study, the authors identified the thermal dynamics of a target house using CTSM-R software and designed a Stratego controller to learn optimal control strategies. The results demonstrated that the intelligent controller saved energy costs while maintaining comfort, ultimately outperforming a traditional bang-bang controller. However, these studies [6, 9, 10] do not consider the buffer tank and mixing loop in the context of domestic heating. We extends these works, and in particular [6], by introducing these components.

Adding a hot water buffer tank to the heating system may improve the control and efficiency of the system. Several studies have examined the simulation and modeling of electric water heaters (EWHs). However, some of these studies, such as [11–22], have only considered a uniform water temperature in the tank and modelled it as a single mass of water using a first-order thermal model. This approach is not effective when there is a hot water out-flow and cold water in-flow in a relatively small buffer tank, as the temperature distribution in the tank tends to be uneven. Two and three-mass [23–25] models have been developed to overcome the limitations of one-mass models. These models assume a constant temperature profile within each water mass, resulting in improved accuracy in calculating the tank water temperature. However, there is still a need for more precise models to capture nonuniform temperatures in the tank effectively. The approaches proposed in [26, 27] discuss how the water temperature in the buffer tank can be calculated with reasonable accuracy. The approaches propose dividing the tank water into several virtual layers to accommodate stratification created due to the temperature difference in different tank areas. Our buffer tank modelling approach is similar to [26, 27], however, they use a simple boiler and we use a heat pump together with intelligent control to heat-up the water.

Furthermore, a mixing loop can be added to adjust the forward water temperature by mixing hot district heating water with cold returning domestic heating water, lowering energy costs [28]. Similarly, the mixing loop modelling methodologies proposed in [29–32] reduce energy costs in low-temperature district heating. Instead of district heating, we propose a mixing loop model together with its intelligent control for an individual house and extensively evaluate the interplay between the buffer tank and the mixing loop.

We believe that we are the first to study the impact of combined intelligent predictive control of both the heat-producing unit and the mixing loop in a buffer-tank-enabled heating system.

2 Case House and Problem Statement

To evaluate the performance of the buffer tank and mixing loop, we now present an overview of the house used in our experiments and the evaluation environment. Figure 1 extends the setup of a small family house modelled in [6] with two additional components: a hot water tank and a mixing loop. It is a $150m^2$ physical test house with four rooms, including a living room with a built-in kitchen (Room 1), two bedrooms (Rooms 2 and 4), and a bathroom (Room 3).

The heat pump system produces hot water and directs it to the buffer tank. This hot water is then distributed to the floor heaters through floor pipes to meet the heating demands of the house. With a buffer tank, the control of heat becomes more indirect. In order to provide better direct control, we integrate a mixing loop between the buffer tank and the floor heaters.

The system has three levels of control, i.e., heat pump, mixing loop, and room thermostat. We consider traditional bang-bang controller to control the room thermostats. Each thermostat operates independently of the heat pump

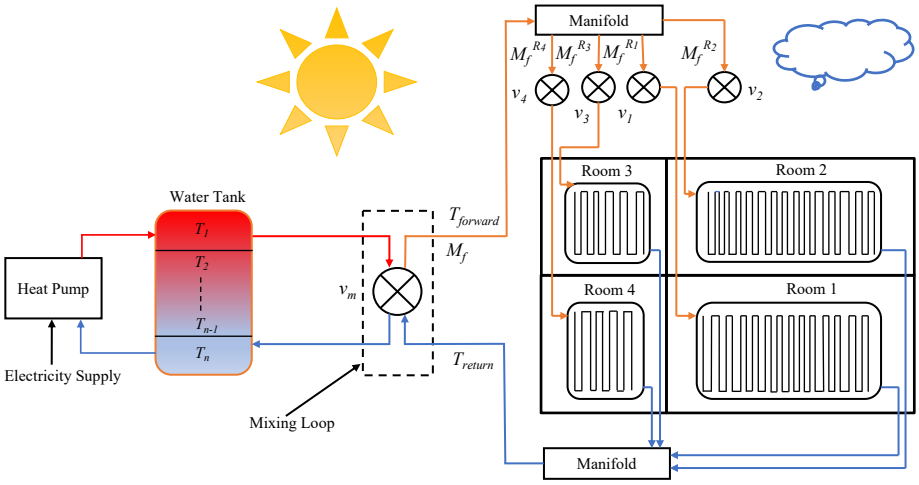

Fig. 1: The overview of the house and its heating system

and other thermostats; it is turned on if any room's temperature drops below the fixed set point (22 °C) and turned off if all the room temperatures exceed it. The incoming mass flow of water (M_f) has a fixed distribution key that distributes the hot water to the rooms via the manifold in fixed proportions denoted by ${M_f}^{R_i}$ where $i = 1, \ldots, k$ (k denotes the number of rooms). Individual room thermostats regulate binary valves v_i, with mass flow re-distributed proportionally to the remaining open valves if certain valves are shut. On the other hand, the heat pump and the mixing loop are controlled with a dedicated controller (e.g., UPPAAL STRATEGO [8] in our case). The control parameters for the heat pump and the mixing loop are the heat pump's operating intensity and level of mixing (through the valve v_m). The objective is to control the heat pump and the mixing loop to achieve optimal comfort and cost. The $T_{forward}$ and T_{return} represent forward and return water temperatures, respectively.

For the modelling purposes and the construction of a predictive controller of the heat pump and the mixing loop, we need to obtain the house's thermodynamic model. We extend the methodology proposed in [6] where the data recorded from the intended house (from OpSys Project [33]) modelled in DYMOLA [34] is used to determine the thermal model of the house, as well as related heat exchange coefficients.

3 Buffer Tank and Mixing Loop Thermodynamics

This section describes our proposed thermal dynamic models of the buffer tank and the mixing loop. In Figure 2a, we present the schematic overview of the hot water buffer tank. We split the tank water into n virtual layers. The temperature of each layer is affected by the direction of the water pressure created either from

Table 1: List of variables and constants used in tank thermodynamic model

Variables	**Description**
$\tilde{T}_1 \cdots \tilde{T}_n$	temperatures of the n water layers in tank[°C]
T_{hp}	temperature of the water exiting the heat pump [°C]
T_{return}	temperature of the water returning from the room floors [°C]
$T_{outdoor}$	ambient temperature [°C]
F_{hp}	mass flow of water exiting the heat pump [litres/minute]
F_{fh}	mass flow of water exiting the floors to the tank [litres/minute]
$F_{(x,y)}$	mass flow of water from layer x to layer y [liters/minute]
Constants	
M	mass of water in each layer [litres]
A	area of each layer [m^2]
C_w	thermal capacitance in the water tank [J/kgC]
U_a	coefficient for heat conductivity to ambient
U_v	coefficient for heat conductivity in the tank water

top-to-bottom or bottom-to-top inside the tank, which is decided by the mass flows from the heat pump (F_{hp}) and to the floors (F_{fh}).

In Figure 2b, we present thermal dynamics model of the buffer tank as a set of differential equations (Equations (1)-3)) representing the temperature of the top layer ($\tilde{T}_1$), finite number of intermediate layers ($\tilde{T}_\ell$), and the bottom layer ($\tilde{T}_n$). In these equations, the heat supply, thermal conductance of the water, and heat loss to the surrounding environment determine the heat balance. The related variables and constants are described in Table 1.

Equation (2) computes the water temperature ($\tilde{T}_\ell$) of any intermediate layer ℓ. The function $f(\ell)$ computes the heat effect (relative to mass flow $F_{(x,y)}$) to and from the layer $\ell-1$ or $\ell+1$ depending on the mass flows F_{hp} and F_{fh}. Whenever F_{hp} is greater than F_{fh}, water pressure is formed from the top to the bottom, causing direct heat gain from the adjacent upper layer $\ell - 1$ and heat loss to the adjacent lower layer $\ell + 1$. In contrast, when F_{fh} is greater than F_{hp}, the water creates pressure from the bottom to the top layer, resulting in a direct heat effect transferring from the adjacent lower layer $\ell + 1$ to ℓ, and from ℓ to $\ell - 1$. The second term calculates the heat loss incurred by the outside weather (related to the coefficient U_a). The fourth and fifth terms express the conductivity impact of the adjacent upper $(\ell - 1)$ and lower layers' $(\ell + 1)$ temperatures on the current layer (ℓ) (through the conductivity coefficient U_v). Equations (1) and (3) are specialized forms of Equation (2) and determine the temperatures $\tilde{T}_1$ and $\tilde{T}_n$. The hot water temperature (T_{hp}) entering the tank greatly influences the top layer. On the other hand, the direct heat influence on the bottom layer is caused by the return water temperature (T_{return}).

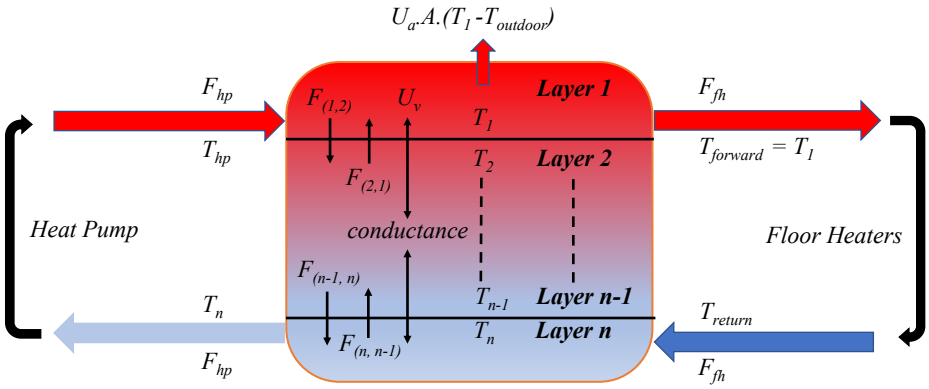

(a) Overview of the hot water buffer tank

$$\frac{d\tilde{T}_1}{dt} = ((F_{hp} \cdot C_w \cdot T_{hp}) - (F_{fh} \cdot C_w \cdot \tilde{T}_1) + f(1) \\ - (U_a \cdot A \cdot (\tilde{T}_1 - T_{outdoor})) + (U_v \cdot (\tilde{T}_1 - \tilde{T}_2)))/(M \cdot C_w) \quad (1)$$

for every ℓ, $2 \leq \ell < n$, *we have the following equation* :

$$\frac{d\tilde{T}_\ell}{dt} = (f(\ell) - (U_a \cdot A \cdot (\tilde{T}_\ell - T_{outdoor})) \\ - (U_v \cdot (\tilde{T}_{(\ell-1)} - \tilde{T}_\ell)) + (U_v \cdot (\tilde{T}_\ell - \tilde{T}_{(\ell-1)})))/(M \cdot C_w) \quad (2)$$

$$\frac{d\tilde{T}_n}{dt} = ((F_{fh} \cdot C_w \cdot T_{return}) - (F_{hp} \cdot C_w \cdot \tilde{T}_n) + f(n) \\ - (U_a \cdot A \cdot (\tilde{T}_n - T_{outdoor})) - (U_v \cdot (\tilde{T}_{n-1} - T_n)))/(M \cdot C_w) \quad (3)$$

where

$$f(1) \coloneqq \begin{cases} -(F_{(1,2)} \cdot C_w \cdot \tilde{T}_1) & \text{if } F_{hp} > F_{fh} \\ +(F_{(2,1)} \cdot C_w \cdot \tilde{T}_2) & \text{otherwise} \end{cases}$$

$$f(\ell) \coloneqq \begin{cases} +(F_{(\ell-1,\ell)}) \cdot C_w \cdot \tilde{T}_{\ell-1}) - (F_{(\ell,\ell+1)} \cdot C_w \cdot \tilde{T}_\ell) & \text{if } F_{hp} > F_{fh} \\ +(F_{(\ell,\ell+1)}) \cdot C_w \cdot \tilde{T}_{\ell+1}) - (F_{(\ell,\ell-1)} \cdot C_w \cdot \tilde{T}_\ell) & \text{otherwise} \end{cases}$$

$$f(n) \coloneqq \begin{cases} +(F_{(n-1,n)} \cdot C_w \cdot \tilde{T}_{n-1}) & \text{if } F_{hp} > F_{fh} \\ -(F_{(n,n-1)} \cdot C_w \cdot \tilde{T}_n) & \text{otherwise} \end{cases}$$

(b) Thermodynamics model of the hot water buffer tank

Fig. 2: Buffer tank schematic diagram and thermal equations for n layers

To evaluate the Equations (1)–(3), we let the buffer tank heat up (charging) and cool down (discharging) to see how the tank water temperatures evolve. To do so, we set the outdoor temperature ($T_{outdoor}$) and tank water's initial temperature to 10 °C and 30 °C, respectively. For simplicity, we limit the virtual

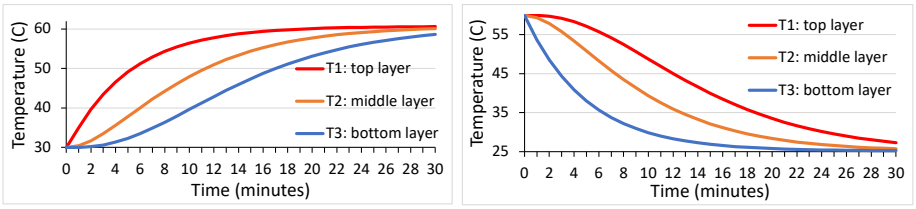

(a) Charging (b) Discharging

Fig. 3: Temperatures of buffer tank water during charging/discharging

layers to three (i.e., $\tilde{T}_1$, $\tilde{T}_2$, and $\tilde{T}_3$) and assume a 75-litre tank size. Figure 3a shows the temperature trends for all three layers during the charging period (30 minutes). The heat pump consumes 2.5 kWh of electricity and supplies hot water to the tank from the top layer at a rate of 5 litres per minute (F_{hp}). However, we restrict the hot water from flowing towards the floor heaters, i.e., $F_{fh} = 0$. The tank water temperatures keep rising, and the gap between them decreases as the heat pump keeps providing the hot water. After a while, the temperatures reach the same point, and no further heat exchange occurs.

During discharging phase (Figure 3b), we keep the heat pump off, and the floor heaters get 5 litres per minute of hot water from the top layer. However, the cold water (T_{return} is 25 °C) returns to the tank via the bottom layer. Due to the continuous infusion of cold water, the layers' temperatures keep dropping and, after some time, become constant at 25 °C.

Finally, we present the thermal model of the mixing loop. The mixing is done with a mixing valve (v_m in Figure 1). Assuming that the *control_choice* is the mixing option selected by the controller from the available mixing levels (*mixing_levels*), the percentage of cold water (*mixing_value*) to be mixed with the hot water can be calculated using Equation (4). Equation (5) computes the temperature of the water to be forwarded ($T_{forward}$) towards the floor heaters using the relative share of cold (T_{return}) and hot water (T_1, top layer). The mass flow of cold water entering the buffer tank (F_{fh}) is calculated using Equation (6).

$$mixing\_value = \frac{control\_choice}{mixing\_levels} \tag{4}$$

$$T_{forward} = T_{return} \cdot mixing\_value + T_1 \cdot (1 - mixing\_value) \tag{5}$$

$$F_{fh} = F_{fh} \cdot (1 - mixing\_value) \tag{6}$$

4 System Modelling in Uppaal Stratego

Given the thermal dynamics model of the buffer tank, we now create its model in Uppaal. We employ the tool Uppaal Stratego [8], which is a branch of the Uppaal tool suit [35–38]. In Stratego, systems are modelled as networks of finite-state automata equipped with discrete data types (e.g., bounded integers,

arrays) and a finite number of clocks (continuous variables). Transitions in the automata are conditioned on the values of the discrete variables and clocks and when executed, both the discrete variables and clocks can be updated. The transitions can be controllable (represented by solid lines) or uncontrollable (represented by dashed lines) guarded with specific conditions. If two parallel processes reach a controllable and uncontrollable transition simultaneously; the environment has priority to take any transition or pass control over to the controller. The clocks facility in STRATEGO captures the timing aspects of the real systems and serves as continuous variables to represent differential equations. Moreover, STRATEGO enables communication with C libraries [39], making it possible to use a C library to write complex functions and interact with other libraries.

4.1 Buffer Tank Modelling in UPPAAL STRATEGO

Figure 4 depicts the complete system composition as a buffer tank in STRATEGO. In STRATEGO, the sub-parts of the model are named templates. The model comprises seven parameterized automata templates, namely *Room*, *Controller*, *FitnessFunction*, *DataReader*, *BufferTank*, *BufferLayer*, and *BufferUpdate*. The continuous variables $\tilde{T}_r^i$, $\tilde{T}_h^i$, and $\tilde{T}_e^i$ representing room, floor, and envelope temperature (for Room i) are expressed as real-time clocks in the *Room* template. *DataReader* brings historical *weather* and day-ahead *electricity* pricing information into the model. The *Fitness* function (see Equation (7)) is implemented by the *FitnessFunction* template. The *Controller* template implements the controller's control mechanism, which allows the system to choose between different energy levels for the heat pump and different valve settings for the mixing loop. The current work focuses mainly on describing the modelling of the buffer tank, so we here explain only the buffer tank-related templates. The complete model with details of the remaining templates can be found on GitHub [40].

The buffer tank-related templates are grouped within the red dashed-line area (see Figure 4a). The *BufferTank* template incorporates two continuous variables (called clocks) to represent the temperature of the top ($\tilde{T}_1$) and bottom ($\tilde{T}_n$) layers, which evolve with time. On the other hand, the *BufferLayer* template calculates the temperature of an arbitrary number of intermediate ($\tilde{T}_\ell$) water layers. The functions `calculate_top()`, `calculate_layer()`, and `calculate_bottom()` employ Equations (1), (2) and (3) to compute $\tilde{T}_1$, $\tilde{T}_\ell$, and $\tilde{T}_n$, respectively. In Figure 4c, we show `calculate_top()` definition as an example to highlight the one-to-one mapping of these functions with buffer tank thermal equations (Equation (1) in this case). The invariant `t≤min` and guard `t≥min` in *BufferUpdate* template combinely force the system (every minute) to take the uncontrollable transition and update the functions `conductivity()`, `massflows_hp_fh()` and reset the local clock `t`. These functions are defined in Figure 4d, while their declarations are presented in Figure 4b. The number of layers, volume, and area of the tank is defined by external calls to the functions in external C libraries.

In Figure 4d, the `conductivity()` function calculates the water mass flow ($\mathsf{F_{xy}}$) between any two consecutive layers by computing the difference of $\mathsf{F_{hp}}$ and $\mathsf{F_{fh}}$. The `massflows_hp_fh()` function is responsible for determining the

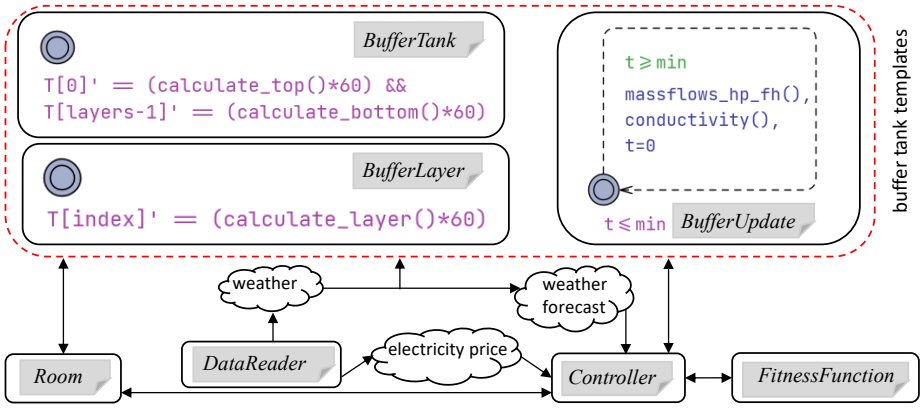

(a) Overall system composition

```
const double M=volume/layers;
const double Cw= 4180.0;
double Fhp= 0.3267;
double Ffh= 0.3267;
double Fxy;
const double Uv=0.6;
const double Ua= 1.5;
const double A=area/layers;
double Thp;
clock T[layers];
typedef int[1,layers-2] mid_t;
const int rooms = 4;
typedef int [0, rooms-1] id_t;
// Layers between top and bottom
const mid_t index;
// Constant mass flow for each room
double massflow[rooms]=
      {0.157, 0.1051, 0.0224, 0.0422};
bool is_mass_flow_on[rooms]=[1,1,1,1];
// Heat pump energy consumption
double consumed_power;
// Heat pump produced heat
double heat_produced;
```

(b) Global declarations

```
double calculate_top(){
    double F;
    if (Fhp > Ffh)
        f = - (Fxy*Cw*T[0]);
    else f = (Fxy*Cw*T[1]);
    return ((Fhp*Cw*Thp)-(Ffh*Cw*T[0])
          + f-(Ua*A*(T[0] - Toutdoor))
          + (Uv*(T[0] -T[1])))/(M*Cw);
}
```

(c) Top layer function

```
void conductivity(){
   if(Fhp > Ffh){
       Fxy = Fhp - Ffh;
   }
   else{
       Fxy = Ffh - Fhp;
   }
}
void massflows_hp_fh(){
   double temp2 = 0.0;
   double temp = 0.0;
   for( r : id_t)
   {
       temp = massflow[r]*is_massflow_on[r];
       temp2 = temp2+temp;
   }
   if(temp2 == 0.0){
       Ffh = 0.0;
   }
   else{
       Ffh = temp2;
   }
   // when heat pump is off
   if (consumed_power == 0.0){
       Fhp = 0.0001;
   }
   // when heat pump is on
   else{
       Fhp = 0.0297 + ((consumed_power
                   -0.625)/0.1875)*0.0297;
   }
   Thp = (heat_produced*1000)/(Fhp*Cw)
                              +T[levels-1];
}
```

(d) Conductivity and mass-flow functions

Fig. 4: Composition of the complete system in STRATEGO

F_{hp} and F_{fh} values. The `massflow[]` and `is_massflow_on[]` arrays used in the *for loop* contain the constant mass flows for each room and Boolean values representing each room's thermostat's *opening/closing* status, respectively. The

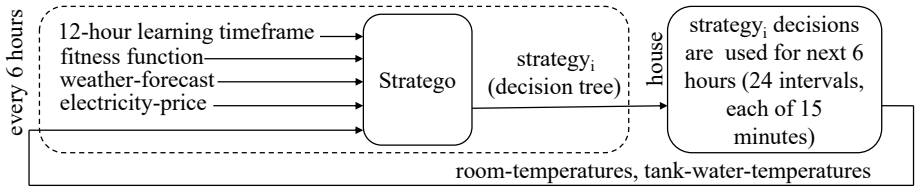

Fig. 5: Online synthesis approach shown on two days period

variable `temp2` adds the contribution of mass flow from each room to determine their combined mass flow $\mathsf{F_{fh}}$ value. However, $\mathsf{F_{hp}}$ depends on the heat pump's intensity, with the maximum value being 0.3267 at full heat pump intensity of 2.5 kWh. Like heat-pump intensity, we split $\mathsf{F_{hp}}$ into equal levels with a value of 0.0297 on each level. The power consumption for the first intensity level is 0.625 kWh, adding 0.1875 kWh against each adjacent intensity level. The function also computes the temperature ($\mathsf{T_{hp}}$) of the water exiting the heat pump.

4.2 Online Synthesis

In Figure 5, we depict an overview of online synthesis algorithm to give a better understanding. Looking further into the future, we see that 24 hours in advance known electricity prices and weather forecasts have diminished predictive power. To address this issue, we propose an online strategy synthesis approach where the controller periodically observes the state of the room, buffer water temperature, electricity price, and weather forecast to learn appropriate control decisions by optimizing the fitness function that balances the comfort and cost. The decisions are generated as a decision tree (i.e., $strategy_i$ in Figure 5 where i represents 6 hours) for operating the heat pump and mixing loop accordingly. The controller uses quick recomputation to compensate for inaccuracies in the initial state. As a result, the volatile variables are monitored and communicated to the strategy $strategy_i$ every 15 minutes to get the control decisions that suit the current situation. A single strategy is used for the subsequent 24 intervals (6 hours) to reduce the computational effort.

5 Experimential Evaluation

We begin by describing the experimental setup and then evaluate our approach by presenting a series of experiments as follows:

1. buffer tank quality assessment with an industry-standard controller,
2. buffer tank evaluations with intelligent STRATEGO controller,
3. buffer and mixing loop evaluations with intelligent STRATEGO controller.

5.1 Evaluation Setup

In our experiments, we control the heat pump from the STRATEGO model for February (week 6) and April (week 14) of 2018 while maintaining corresponding weather conditions. For all trials described in the following sections, we use the energy prices from the Danish day-ahead electricity market as of autumn 2022.

We optimize the control mechanism against the *objective/fitness* function (in Equation 7, which is similar to one introduced in [6]). The fitness function (F) provides flexibility to handle the tradeoff between cost and comfort in a balanced way by adjusting the relative weights. Typically, a consumer wishes to manage the tradeoff between cost and comfort by adjusting the weight against each parameter. Therefore, we state the optimization criteria that allow the customer to perform such tuning with $0 \leq W_{comf} \leq 1$ weighting factor. This encourages us to express the fitness function for our controllers parameterized as W_{comf}. For each W_{comf} setting, W_{cost} is compted as $W_{cost} = 1 - W_{comf}$. To ensure proportional weighting between two units, cost (DKK), and squared degrees Celsius, we calculated a normalization factor, *norm*, based on the performance of the traditional bang-bang (BB) controller. The controller simply turns the heat pump on if the temperature in any room falls below 22°C and turns it off otherwise. We calculated the normalization factor by assessing the performance of the BB controller in terms of cost and comfort in the week preceding the experimental week using the formula $norm = \frac{comfort}{cost}$. The main purpose of the heat pump is to minimize the gap between the room temperatures $\tilde{T}_r^i$ and a given set point T_g with the heating cost. The heating cost $cost(\tau) = price_\tau \cdot w_\tau$ is a time-dependent function and product of the heat pump energy consumption w_τ (determined directly by the controller) and the hourly basis (known 24 hours in advance) market electricity price ($price_\tau$). We apply the function over a period τ_0 to τ_n given that the heat-pump settings, energy prices, and room temperatures (denoted by $T_r^i(\tau)$) are known for k rooms:

$$F(\tau_0, \tau_n) = \int_{\tau_0}^{\tau_n} \left((W_{cost} \cdot norm \cdot cost(\tau)) + W_{comf} \cdot \sqrt{\sum_{i=1}^{k} (T_g - \tilde{T}_r^i(x))^2} \right) d\tau \tag{7}$$

where the first part represents the energy cost (linear impact on fitness), and the second part records the room temperature deviations (from the set point (T_g)) such that the large deviations are penalized substantially as compared to minor deviations due to its squared manner.

We limit the controller to 15-minute control intervals, which is enough for systems with slow dynamics, such as floor heating. Each reported configuration is tested ten times, and the mean value and standard deviation intervals are displayed in bar charts. Throughout the study, W_{comf} values are changed in 0.1 increments.

5.2 Buffer Tank Quality Assessment

In this section, we analyze the buffer tank size and the number of virtual layers that are sufficient to calculate the water temperature within the tank with adequate accuracy. Selecting the buffer tank's proper size can save installation and operation costs. A too small buffer tank sometimes needs more storage capacity to fulfil the heating demand of the heating system. The limited capacity enforces the heat pump for frequent cycling and may reduce system efficiency. On the other hand, too large buffer tanks need higher installation costs and may cause significant heat losses. Another interesting aspect is the precision of the buffer tank, which is affected by the number of virtual layers.

To investigate these issues, we use a heat pump control strategy presented in the reference curve of an industry-standard product sheet [41]. The product sheet proposes regulating the forward water temperature according to outside weather for a heat pump with no buffer; however, regulating return water temperature instead ensures reasonable forward temperatures for a heat pump with a buffer tank. Therefore, we implement this strategy to operate the heat pump based on the return water temperature (T_{return}). The strategy turns on the heat pump if the return water temperature drops below 50 °C and turns it off if it exceeds 55 °C. We name this strategy as Return Water Control Strategy (RWCS-BT, where BT refers to buffer tank).

Now we consider February (week 6) to examine the influence of tank sizes and levels on the performance of a heat pump under the control of the RWCS-BT controller, equally focusing on cost and comfort. The investigation utilizes a simulation horizon of one week, with a target temperature of 22 °C. Figure 6 displays the experiment results. The vertical axis displays the absolute values of the fitness function, energy cost (in DKK) and discomfort, where discomfort records the room temperature deviations from the target temperature. Figures 6a, 6b, and 6c illustrate the impact of tank sizes concerning fitness, discomfort and cost using the test house from Section 2. Our findings suggest that increasing the tank size leads to a decrease in discomfort and a rise in cost, with the improvement in comfort being relatively less significant than the corresponding increase in energy cost. The increase in cost is attributed to the greater heat dissipation to the surrounding environment that arises when larger tanks are considered. Fitnesswise 150-litre option is better than the 75-litre; however, the 75-litre tank is the most cost-effective option, exhibiting an approximately similar level of discomfort compared to other tank sizes. The 75-litre tank size can also save the installation cost significantly compared to the 150-litre tank. As a result, we employ the 75-litre tank in subsequent experiments.

In Figure 6d, we investigate the impact of virtual layers in a buffer tank. We observe that the fitness value increases up to 7 layers and becomes stable afterwards. Therefore, we conclude that the 7 virtual layers give sufficient precision for a 75-litre tank. As a result, we have decided to employ the 7 virtual layers in 75 litres tank in subsequent sections of this paper. We note that the precision of the buffer tank is dependent on many factors, e.g., the size of the buffer tank and operational circumstances (i.e., heat pump dimensionality and user patterns).

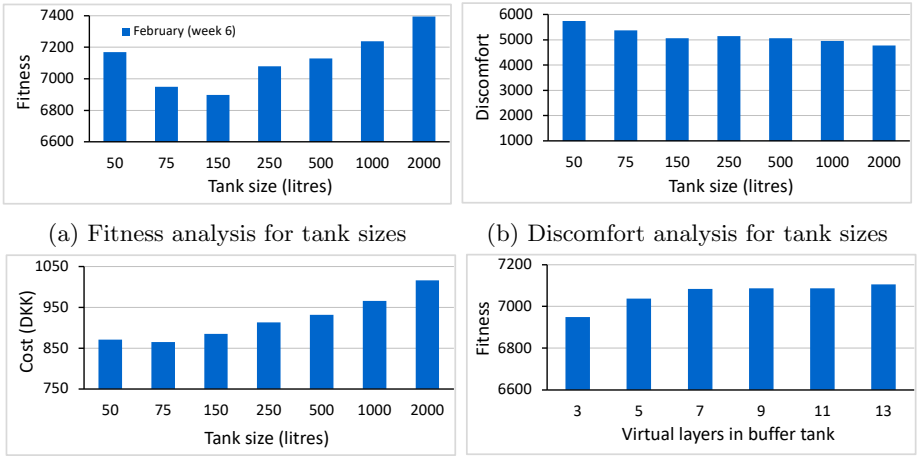

(a) Fitness analysis for tank sizes

(b) Discomfort analysis for tank sizes

(c) Cost analysis for tank sizes

(d) Fitness analysis for virtual layers

Fig. 6: The effect of tank sizes and virtual layers on the cost and comfort

5.3 Buffer Tank Evaluations with Intelligent STRATEGO Controller

In this section, we discuss the performance of various iterations of the online STRATEGO-based controller. We include random noise (upto 1 °C) in the historical weather data to account for discrepancies in weather information between the house and the controller as the house experiences actual weather and the controller relies on weather forecasts. We introduce several controllers to evaluate our approach:

- BB: It is a traditional bang-bang controller to control the heat pump without a buffer tank. This controller turns the heat pump on if the temperature in any room falls below 22 °C and turns it off otherwise,
- STRATEGO: A predictive controller that trains on the house model to learn good decisions to operate the heat pump. It controls the intensity of the heat pump between 11 levels. Like BB, it operates the heat pump without a buffer tank,
- RWCS-BT: As already described in Section 5.2, it is a controller from industry-standard that maintains the return water temperature between 50-55 °C. It operates the heat pump with a buffer tank.
- STRATEGO-BT: It is also a predictive controller. Like RWCS-BT, this it is designed to control the heat pump with a buffer tank (but no mixing loop).

We consider BB to be the baseline controller because its behaviour in the model is deterministic when repeated with historical weather. The experimental findings of the controllers for April (week 14) control are shown in Figure 7. The fitness and cost measures on vertical axis represent the fitness function (F) and energy cost (in DKK). Discomfort measure, on the other hand, displays the recorded deviations in room temperatures from the set point. Each measure on

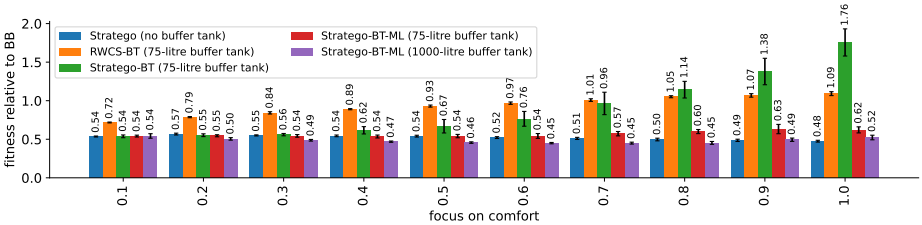

(a) Fitness measured against different W_{comf} settings

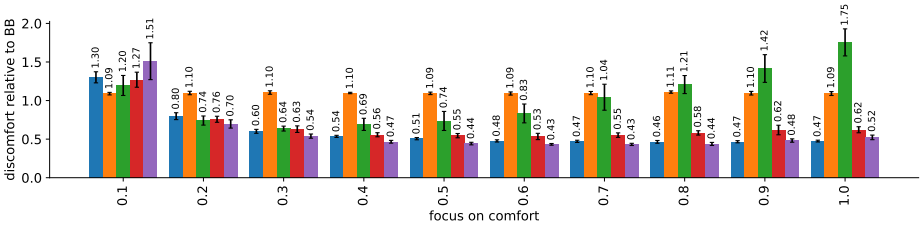

(b) Discomfort measured against different W_{comf} settings

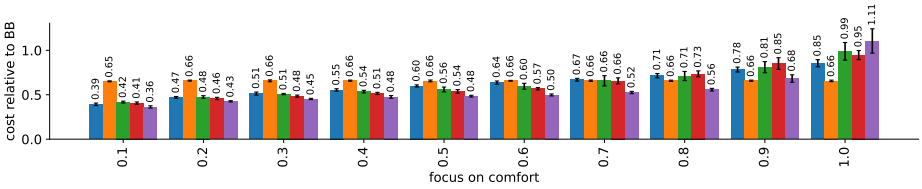

(c) Cost measured against different W_{comf} settings

Fig. 7: Experimental results for April (week 14) control under Stratego-BT-ML

the vertical axis is calculated by computing its value from a specific controller and BB using the formula $measure = \frac{controller}{\text{BB}}$ which means a relative value below 1 implies that a controller outperforms BB and vice versa. The horizontal axis emphasizes comfort (with W_{comf} values). We avoid reporting a pure focus on cost (i.e., $W_{comf} = 0.0$) because it causes the controller to turn off all heat.

Figure 7 shows the comparison of Stratego, RWCS-BT, and Stratego-BT controllers (shown by the first three bar charts i.e., blue, yellow and green) relative to the BB controller. Here Stratego-BT is unexpectedly underperforming Stratego with respect to fitness, comfort, and cost (see Figures 7a, 7b and 7c), especially with more focus on comfort. The higher cost is due to the heat loss from the buffer tank to the ambient. The loss in comfort is attributed to Stratego-BT controller's lack of control over room thermostats; they get activated whenever the temperature in corresponding rooms goes below 22 °C. With an increased focus on comfort, Stratego-BT anticipates heat demand and produces high-temperature hot water in the buffer tank. This water is released when a thermostat valve opens, causing discomfort (overheating). Hence the introduction of a buffer tank without a mixing loop is not benificial.

5.4 Mixing Loop Evaluations with Intelligent STRATEGO Controller

We integrate a mixing loop between the buffer tank and the floor heaters to improve the cost and comfort. We create controller STRATEGO-BT-ML, which controls the heat pump and water mixing proportions, and we experiment with several mixing level settings. Our finding is that 11 mixing levels give the controller enough flexibility to mix hot and cold water appropriately. It can be seen in Figure 7 that STRATEGO-BT-ML (75-litre) outperforms STRATEGO-BT; however, with a higher focus on comfort, it still performs worse than STRATEGO indicating that 75-litre tank is insufficient for optimal mixing loop operation. Therefore, we include a 1000-litre tank that allows the heat pump to store heat when it is cheap and better handle the mixing loop. STRATEGO-BT-ML (1000 litres) consistently outperforms STRATEGO except for extreme cases where we ignore comfort or cost (i.e., W_{comf} at 0.1 or 1.0). For example, with equal focus on comfort and cost ($W_{comf} = 0.5$), it saves 12 % energy costs with 7 % better comfort than STRATEGO. We want to remark here, that these numbers are specific to our case house and may differ for houses with different thermodynamics.

6 Conclusion

We proposed scalable thermal models for the hot water buffer tank and the mixing loop, which we then incorporated into a $150m^2$ test house used in the toolchain from [6]. First, we examined the buffer tank's quality using an industry-standard controller (RWCS-BT). The results suggest that a 75-liter capacity with seven virtual layers is sufficient for adequate heat pump operation.

We compared the performance of RWCS-BT and three intelligent controllers having: no buffer tank (STRATEGO), a buffer tank (STRATEGO-BT), and a buffer tank and a mixing loop (STRATEGO-BT-ML). Our findings reveal that both RWCS-BT and STRATEGO-BT perform worst than STRATEGO in terms of cost and comfort due to the lack of the mixing loop. STRATEGO-BT-ML (75-litre) with a mixing loop mitigates the higher cost and comfort to some extent, but still, it underperforms STRATEGO. However, a 1000-litre tank with a mixing loop enables STRATEGO-BT-ML to outperform all other controllers, saving substantial energy costs while improving comfort. Larger tanks are expensive, but they can save energy by storing heat when it is cheap.

Our method gives a more in-depth understanding of buffer tanks and mixing loops, allowing customers to choose the optimal tank size for their heating requirements. Before purchasing a buffer tank, customers may conduct model-based simulations to explore a variety of different tank sizes under the local weather conditions in order to calculate the possible savings.

Acknowledgements: We would like to thank Per Printz Madsen and Hessam Golmohammadi for their extensive help in understanding the physics of the buffer tanks. This research is partly funded by the ERC Advanced Grant Lasso, the Villum Investigator Grant S4OS, and DIREC: Digital Research Centre Denmark.

References

1. Energy consumption in households. `https://ec.europa.eu/eurostat/statistics-explained/index.php?title=Energy_consumption_in_households`, April 2023.
2. Mohamad K. Daryabari, Reza Keypour, and Hessam Golmohamadi. Stochastic energy management of responsive plug-in electric vehicles characterizing parking lot aggregators. *Applied Energy*, 279:115751, 2020.
3. M. K. Agesen, K. G. Larsen, M. Mikučionis, M. Muñiz, P. Olsen, T. Pedersen, J. Srba, and A. Skou. Toolchain for user-centered intelligent floor heating control. In *IECON 2016 - 42nd Annual Conference of the IEEE Industrial Electronics Society*, pages 5296–5301, 2016.
4. Kim G. Larsen, Marius Mikučionis, Marco Muñiz, Jiří Srba, and Jakob Haahr Taankvist. Online and compositional learning of controllers with application to floor heating. In Marsha Chechik and Jean-François Raskin, editors, *Tools and Algorithms for the Construction and Analysis of Systems*, pages 244–259, Berlin, Heidelberg, 2016. Springer Berlin Heidelberg.
5. P.J.C. Vogler-Finck, R. Wisniewski, and P. Popovski. Reducing the carbon footprint of house heating through model predictive control – A simulation study in Danish conditions. *Sustainable Cities and Society*, 42:558 – 573, 2018.
6. Imran Riaz Hasrat, Peter Gjøl Jensen, Kim Guldstrand Larsen, and Jiří Srba. End-to-end heat-pump control using continuous time stochastic modelling and uppaal stratego. In Yamine Aït-Ameur and Florin Crăciun, editors, *Theoretical Aspects of Software Engineering*, pages 363–380, Cham, 2022. Springer International Publishing.
7. Rune Juhl, Jan Kloppenborg Møller, and Henrik Madsen. CTSMR - Continuous Time Stochastic Modeling in R. *arXiv*, 2016.
8. Alexandre David, Peter Gjøl Jensen, Kim Guldstrand Larsen, Marius Mikučionis, and Jakob Haahr Taankvist. Uppaal stratego. In *International Conference on Tools and Algorithms for the Construction and Analysis of Systems*, pages 206–211. Springer, 2015.
9. Rune Hermansen, Kevin Smith, Jan Eric Thorsen, Jiawei Wang, and Yi Zong. Model predictive control for a heat booster substation in ultra low temperature district heating systems. *Energy*, 238:121631, 2022.
10. Kim G. Larsen, Marius Mikučionis, Marco Muñiz, Jiří Srba, and Jakob Haahr Taankvist. Online and compositional learning of controllers with application to floor heating. In Marsha Chechik and Jean-François Raskin, editors, *Tools and Algorithms for the Construction and Analysis of Systems*, pages 244–259, Berlin, Heidelberg, 2016. Springer Berlin Heidelberg.
11. Arnaldo Sepulveda, Liam Paull, Walid G Morsi, Howard Li, CP Diduch, and Liuchen Chang. A novel demand side management program using water heaters and particle swarm optimization. In *2010 IEEE Electrical Power & Energy Conference*, pages 1–5. IEEE, 2010.
12. Liam Paull, Derek MacKay, Howard Li, and Liuchen Chang. Awater heater model for increased power system efficiency. In *2009 Canadian Conference on Electrical and Computer Engineering*, pages 731–734. IEEE, 2009.
13. Shuai Lu, Nader Samaan, Ruisheng Diao, Marcelo Elizondo, Chunlian Jin, Ebony Mayhorn, Yu Zhang, and Harold Kirkham. Centralized and decentralized control for demand response. In *ISGT 2011*, pages 1–8. Ieee, 2011.

14. M Hashem Nehrir, Runmin Jia, Donald A Pierre, and Donald J Hammerstrom. Power management of aggregate electric water heater loads by voltage control. In *2007 IEEE Power Engineering Society General Meeting*, pages 1–6. IEEE, 2007.
15. Chong Hock K Goh and Jay Apt. Consumer strategies for controlling electric water heaters under dynamic pricing. In *Carnegie Mellon Electricity Industry Center Working Paper*, 2004.
16. M Hashem Nehrir, Runmin Jia, Donald A Pierre, and Donald J Hammerstrom. Power management of aggregate electric water heater loads by voltage control. In *2007 IEEE Power Engineering Society General Meeting*, pages 1–6. IEEE, 2007.
17. PS Dolan, MH Nehrir, and V Gerez. Development of a monte carlo based aggregate model for residential electric water heater loads. *Electric Power Systems Research*, 36(1):29–35, 1996.
18. JC Laurent and RP Malhame. A physically-based computer model of aggregate electric water heating loads. *IEEE transactions on power systems*, 9(3):1209–1217, 1994.
19. IE Lane and N Beute. A model of the domestic hot water load. *IEEE transactions on power systems*, 11(4):1850–1855, 1996.
20. Runmin Jia, M. Hashem Nehrir, and Donald A. Pierre. Voltage control of aggregate electric water heater load for distribution system peak load shaving using field data. In *2007 39th North American Power Symposium*, pages 492–497, 2007.
21. Khalid Elgazzar, Howard Li, and Liuchen Chang. A centralized fuzzy controller for aggregated control of domestic water heaters. In *2009 Canadian Conference on Electrical and Computer Engineering*, pages 1141–1146. IEEE, 2009.
22. Liam Paull, Howard Li, and Liuchen Chang. A novel domestic electric water heater model for a multi-objective demand side management program. *Electric Power Systems Research*, 80(12):1446–1451, 2010.
23. Junji Kondoh, Ning Lu, and Donald J Hammerstrom. An evaluation of the water heater load potential for providing regulation service. In *2011 IEEE Power and Energy Society General Meeting*, pages 1–8. IEEE, 2011.
24. Ruisheng Diao, Shuai Lu, Marcelo Elizondo, Ebony Mayhorn, Yu Zhang, and Nader Samaan. Electric water heater modeling and control strategies for demand response. In *2012 IEEE power and energy society general meeting*, pages 1–8. IEEE, 2012.
25. Xiaochen Yang and Svend Svendsen. Improving the district heating operation by innovative layout and control strategy of the hot water storage tank. *Energy and Buildings*, 224:110273, 2020.
26. Abdul Atisam Farooq, Abdul Afram, Nicola Schulz, and Farrokh Janabi-Sharifi. Grey-box modeling of a low pressure electric boiler for domestic hot water system. *Applied Thermal Engineering*, 84:257–267, 2015.
27. Simon Furbo. Heat storage for solar heating systems. *Educational Note, BYG.DTU U-071, ISSN 1396-4046*, 2005.
28. Hessam Golmohamadi and Kim Guldstrand Larsen. Economic heat control of mixing loop for residential buildings supplied by low-temperature district heating. *Journal of Building Engineering*, 46:103286, 2022.
29. Anders Overgaard, Brian Kongsgaard Nielsen, Carsten Skovmose Kallesøe, and Jan Dimon Bendtsen. Reinforcement learning for mixing loop control with flow variable eligibility trace. In *2019 IEEE Conference on Control Technology and Applications (CCTA)*, pages 1043–1048, 2019.
30. Anna Volkova, Igor Krupenski, Aleksandr Ledvanov, Aleksandr Hlebnikov, Kertu Lepiksaar, Eduard Latõšov, and Vladislav Mašatin. Energy cascade connection of

a low-temperature district heating network to the return line of a high-temperature district heating network. *Energy*, 198:117304, 2020.
31. Wiebke Meesenburg, Torben Ommen, Jan Eric Thorsen, and Brian Elmegaard. Economic feasibility of ultra-low temperature district heating systems in newly built areas supplied by renewable energy. *Energy*, 191:116496, 2020.
32. Ali Rahmatmand, Marin Vratonjic, and Pierre E. Sullivan. Energy and thermal comfort performance evaluation of thermostatic and electronic mixing valves used to provide domestic hot water of buildings. *Energy and Buildings*, 212:109830, 2020.
33. Søren Østergaard Jensen. OPSYS tools for investigating energy flexibility in houses with heat pumps. `https://www.annex67.org/media/1838/report-opsys-flexibilitet.pdf`, 2018.
34. Dayssault systems. dymola (dynamic modeling laboratory) systems engineering). `https://www.3ds.com/products-services/catia/products/dymola/`, October 2022.
35. Kim G Larsen, Paul Pettersson, and Wang Yi. Uppaal in a nutshell. *International journal on software tools for technology transfer*, 1(1-2):134–152, 1997.
36. Gerd Behrmann, Alexandre David, Kim Guldstrand Larsen, John Håkansson, Paul Pettersson, Wang Yi, and Martijn Hendriks. Uppaal 4.0. *IEEE Computer Society*, 2006.
37. Peter Bulychev, Alexandre David, Kim Gulstrand Larsen, Marius Mikučionis, Danny Bøgsted Poulsen, Axel Legay, and Zheng Wang. Uppaal-SMC: Statistical model checking for priced timed automata. *arXiv preprint arXiv:1207.1272*, 2012.
38. Gerd Behrmann, Agnes Cougnard, Alexandre David, Emmanuel Fleury, Kim G Larsen, and Didier Lime. Uppaal-tiga: Time for playing games! In *International Conference on Computer Aided Verification*, pages 121–125. Springer, 2007.
39. Peter Gjøl Jensen, Kim Guldstrand Larsen, Axel Legay, and Ulrik Nyman. Integrating tools: Co-simulation in uppaal using fmi-fmu. In *2017 22nd International Conference on Engineering of Complex Computer Systems (ICECCS)*, pages 11–19. IEEE, 2017.
40. Imran Riaz Hasrat, Peter Gjøl Jensen, Kim Guldstrand Larsen, and Jiří Srba. Complete Uppaal Stratego Model for "Modelling of Hot Water Buffer Tank and Mixing Loop for an Intelligent Heat Pump Control", May 2023. `https://github.com/ImranRiazAAU/BufferTankModelling.git`.
41. Control technology: weather compensated controls (Viessmann: climate of innovation). `https://viessmanndirect.co.uk/files//8e57dbc7-8a10-4065-bcc6-a27700ee752a/weather_comp.pdf`, 2023.